Stability Analysis and Experimental Research of a Flywheel Supported by Active Magnetic Bearings

Kai Zhang, Hongbin Zhao
University of Tsinghua, Department of Engineering Physics Beijing, 100084 China
Lei Zhao, Xingzhong Diao, Suyuan Yu
Institute of Nuclear Energy Technologies, Tsinghua University, Beijing, 100084 China

ABSTRACT

Gyroscopic effects of a flywheel rotor supported by active magnetic bearings greatly influence system stability. Effectively damping the rotor nutation is a challenge for the controller designs of the system. To improve rotational speeds of the rotor, how a PD controller and phase lag factors changed the dynamics and the stability of the rotor in operation was studied. With the phase lag factors in the closed-loop system, effects of the cross feedback control on the nutation stability were studied too. Some simulation results and experiment results are provided. It is shown that the phase lag factors and the PD controller greatly influence the nutation frequency value of the closed-loop system. The real damping of the nutation becomes poor and the nutation frequency increases to near a double-synchronous frequency when the rotor runs at high rotational speeds. Sensor runout signals can excite the nutation vibration and make the rotor unstable. In controller designs, the nutation resonance peak of the closed-loop system near double-synchronous frequency should be avoided. At the same time, the sensor runout signals should be restrained.

INTRODUCTION

Magnetic bearings have been utilized in a wide variety of applications such as high speed trains, centrifugal compressors, grinding machines, reaction and gyroscopic wheels for attitude control of spacecraft, and energy storage wheels, since they have unique advantages of non-contact, elimination of lubrication, low power loss, automatic balancing capability, and controllability of bearing dynamics characteristics [1,2,3,4,5].

The flywheel system mentioned in this paper is to be used in spacecraft and replace a system supported by conventional ball bearings for attitude control. The system can prevent the harmful disturbance comes from ball bearings due to residual imbalance or bearing imperfections.

Magnetic bearings are open-loop unstable which means closed-loop control is necessary for stable operation. Usually, such classical feedback control techniques as PD or PID are used. Of course, more complete control methods should be applied according to practical needs. For examples, the cross feedback control was used to stabilize the flywheel rotor in this application.

When an elastically supported rotor runs at a high rotational speed, the ratio of its nutation frequency to the rotational frequency is near its polar-to-transverse inertia ratio because of gyroscopic effects. The gyroscopic effects of the flywheel rotor greatly influence the system stability. Effectively damping the rotor nutation is a challenge for the controller designs of the system, and poor nutation damping will cause the rotor to be unstable at high rotational speeds. To improve the rotational speed of the rotor, how a PD controller and phase lag factors change the dynamics and the stability of the rotor in operation was studied. With the phase lag factors in the closed-loop system, the effects of the cross feedback control on the nutation stability were studied too. Some simulation results and experiment results are provided. It is shown that the phase lag factors and the PD controller greatly influence the nutation frequency value of the closed-loop system. The real damping of the nutation becomes poor and the nutation frequency increases to near a double-synchronous frequency when the rotor runs at a high rotational speed. At the same time, sensor runout [6] signals can excite nutation vibrations of the rotor and make it unstable. In controller designs, the nutation of the closed-loop system and the sensor runout signals should be considered carefully to avoid unstable vibrations.

MODEL

Major parameters of the flywheel system are given in Table 1.

TABLE 1 Momentum wheel data

Item	Note
Bearing	5 DOF AMBs
Angular momentum	100 kg·m^2/s
Rotation speed	20 000 r/min
Mass	13 kg
Inertial moment	0.065 kg·m^2
Power consumption	50 W

For the flywheel system, the axial direction of the rotor is assumed to be decoupled with the radial directions [1]. So the positions of the axial directions can be controlled by conventional PID controllers, this paper only models the rotor in radial directions and analyzes its dynamics behavior. The simple structure of the system is shown in Figure 1.

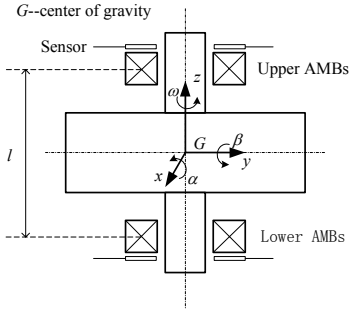

FIGURE 1: Simple structure of the flywheel system.

To simplify the problem, the following assumptions are made:

1) The magnetic force linearization condition is satisfied

[1].

2) A rigid body model of the rotor is used to discuss the behavior of the rotor at different rotational speeds.
3) For the radial AMBs, isotropic suspension is assumed.
4) The rotor is symmetrical about all its principal axes (x-axis, y-axis and z-axis).

The rotor's dynamics equations are established based on the assumptions above.

Furthermore, the phase lag factors in the closed-loop system have to be considered in actual analysis of the system behavior. They include several aspects as follows:

1) Delay of magnetic forces [1]
2) Delay of sampling and holding
3) Delay of amplifiers
4) Delay of the eddy-current sensors
5) Delay of the notch filters in the controllers

The delay factors are finally simplified as a low-pass filter—1/ (Ts+1) (T is set to 0.0005 s).

DYNAMICS ANALYSIS

Some necessary symbol definitions are given as follows:

J_p inertial moment of the rotor about the z-axis
J_d inertial moment of the rotor about the x-axis or the y-axis
i imaginary number
m mass of the rotor
ω rotational speed of the rotor
l distance between the two radial AMBs
k stiffness of the AMBs' suspension
D differentiator coefficient
k_c displacement cross feedback parameter
k_v velocity cross feedback parameter
x displacement along the x direction
y displacement along the y direction

The coordinate of the rotor is illustrated in figure 1. For this model, the rotor's translational and angular modes are uncoupled, and the basic behavior is easier to be discussed.

1. ELASTIC SUSPENSION

First, the rigid rotor with the same elastic suspension at the two radial AMBs was studied as the basis of subsequent discussions. The motion equations of the rotor are given as follows [7, 8]:

$$J_d \ddot{\alpha} + J_p \omega \dot{\beta} + 0.5kl^2 \alpha = 0 \quad (1)$$

$$J_d \ddot{\beta} - J_p \omega \dot{\alpha} + 0.5kl^2 \beta = 0 \quad (2)$$

$$m_r \ddot{x} + 2kx = 0 \quad (3)$$

$$m_r \ddot{y} + 2ky = 0 \quad (4)$$

The solution of the equations shows that the nutation frequency ω_n increases with the rotational speed ω(when ω tends to infinite, ω_n will be $(J_p/J_d)\,\omega$. The value of J_p to J_d is about 1.6 here) whereas the precession frequency ω_p decreases (when ω tends to infinite, ω_p will be zero). When the stiffness of the suspension is 0.2 N/um, the eigenfrequencies corresponding to the nutation and the precession in function of the rotational speed is shown in Figure 2.

It is seen that the ratio of the inertial moments is a determining factor of the nutation frequency.

Now, with the low-pass filter in the proportional

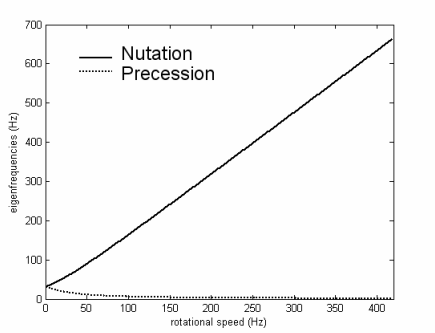

FIGURE 2: eigenfrequencies corresponding to the nutation and the precession in function of the rotational speed.

feedback, Equation (1) and (2) become as follows:

$$J_d \ddot{\alpha} + J_p \omega \dot{\beta} + 0.5kl^2 \int_{-\infty}^{+\infty} \alpha(\tau) F_{ilter}(t-\tau) d\tau = 0 \quad (5)$$

$$J_d \ddot{\beta} - J_p \omega \dot{\alpha} + 0.5kl^2 \int_{-\infty}^{+\infty} \beta(\tau) F_{ilter}(t-\tau) d\tau = 0 \quad (6)$$

From the above equations, the following equation can be gotten:

$$J_d(\ddot{\alpha} + i\ddot{\beta}) - J_p \omega i(\dot{\alpha} + i\dot{\beta}) + 0.5kl^2 \int_{-\infty}^{+\infty} (\alpha(\tau) + i\beta(\tau)) F_{ilter}(t-\tau) d\tau = 0 \quad (7)$$

Defining $\varphi = \alpha + i\beta$, the following equation can be derived from (7):

$$J_d \ddot{\varphi} - J_p \omega_0 i \dot{\varphi} + 0.5kl^2 \int_{-\infty}^{+\infty} \varphi(\tau) F_{ilter}(t-\tau) d\tau = 0 \quad (8)$$

Taking the Laplace Transform for the above equation leads to the eigenequation as follows:

$$J_d s^2 - J_p \omega_0 i s + 0.5kl^2 / (Ts+1) = 0 \quad (s = (\xi + i)\omega) \quad (9)$$

The solotion of the above equation shows that the low-pass filter changes the eigenfrequency values only a little. The eigenfrequency values at zero rotation are different with or without the low-pass filter, because the low-pass filter alters the stiffness of the system. The nutation frequency of the rotor with the low-pass filter considered is a little lower.

The low-pass filter harms the damping of the nutation and the precession, and cause the damping to decrease, especially for the nutation of the rotor. The nutation and the precession become one of the unstable factors of the rotor.

2. WITH DIFFERENTIATORS

If differentiators are added to damp the gyroscopic motions, equations (1) and (2) become as follows:

$$J_d \ddot{\alpha} + J_p \omega \dot{\beta} + 0.5Dl^2 \dot{\alpha} + 0.5kl^2 \alpha = 0 \quad (10)$$

$$J_d \ddot{\beta} - J_p \omega \dot{\alpha} + 0.5Dl^2 \dot{\beta} + 0.5kl^2 \beta = 0 \quad (11)$$

If $\varphi = \alpha + i\beta$ is defined, the above equations can be written as follows:

$$J_d \ddot{\varphi} + (0.5Dl^2 - J_p \omega i)\dot{\varphi} + 0.5kl^2 \varphi = 0 \quad (12)$$

Its eigenequation can be deduced as follows:

$$J_d s^2 + (0.5Dl^2 - J_p \omega i)s + 0.5kl^2 = 0 \quad (13)$$

Its latent roots are given as:

$$s = \frac{(J_p \omega i - 0.5Dl^2) \pm \sqrt{(0.5Dl^2 - J_p \omega i)^2 - 2J_d kl^2}}{2J_d} \qquad (14)$$

From the above derivation (D = 0.004 N·s/um), the eigenfrequencies in function of the rotational speed can be seen in Figure 3.

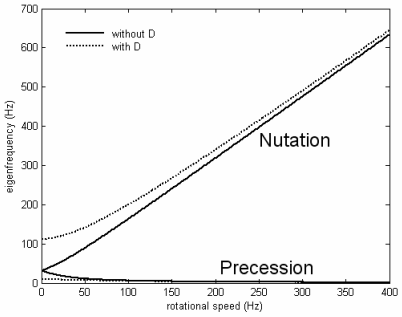

FIGURE 3: Eigenfrequencies in function of the rotational speed.

In Figure 3, it can be found that the D greatly changes the eigenfrequency values at low rotational speeds while it only slightly changes the eigenfrequency values at high rotational speeds. Furthermore, the D greatly influences the damping of the nutation and the damping of the precession. The damping of both of the motion decreases as rotational speed increases, and it will become zero when the rotational speed tends to infinite.

But the differentiators in (10), (11) are both ideal differentiators. Applying such differentiators increases high frequency noise and makes the system unstable. Furthermore, the phase lag factors mentioned in the previous sections also influences the differentiators. Here, a first order differentiator is used to illustrate the problem.

Replacing the D with D/(Ts+1) results in the following equation with the similar derivation as (15):

$$J_d s^2 - J_p \omega i s + 0.5Dl^2 s/(Ts+1) + 0.5kl^2 = 0 \qquad (s = (\xi + i)\omega) \qquad (15)$$

With $0.5Dl^2 s/(Ts+1)$ (T=0.0002 s), the eigenfrequencies in function of the rotational speed are illustrated in Figure 4.

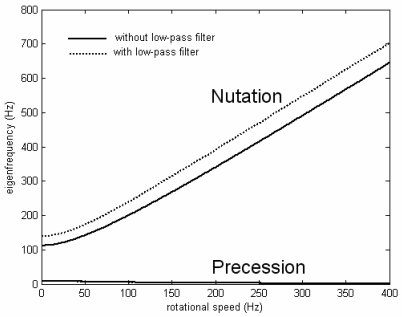

FIGURE 4: eigenfrequencies in function of the rotational speed.

Figure 4 shows that the nutation frequency increases noticeably and the ratio of the nutation frequency to the synchronous frequency at high rotation speeds is no longer close to 1.6 but is much higher. The precession frequency is influenced only a little.

With T=0.0002 s, the damping of the eigenfrequencies in function with the rotation speed is shown in Figure 5. It is seen that the damping of the nutation and the damping of the precession decrease while the rotational speed increases.

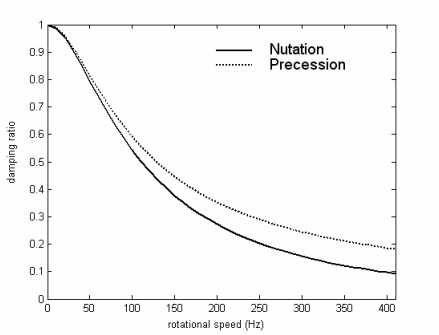

FIGURE 5: Damping of the eigenfrequencies in function with the rotation speed.

3. CROSS FEEDBACK CONTROL

The cross feedback control adds cross feedback channels to PD controllers. We have given detailed discussion of the dynamics influences of the cross feedback control in a previous paper [9]. The conclusion is that the displacement cross feedback helps restraint of the precession but hinders restraint of the nutation and it has little effect on the eigenfrequencies of the rotor, whereas the velocity cross feedback can restrain the gyroscopic motions and decrease the nutation frequency while increasing the precession frequency [10].

However, in that paper [9], the phase lag factors in the cross channels of the controllers had not yet been studied, and they will be discussed below.

For the displacement cross feedback control, the eigenequation with the low-pass filter is given as follows:

$$J_d s^2 - J_p \omega i s + (0.5kl^2 - k_c i)/(Ts+1) = 0 \qquad (16)$$

The solution of Eq. 16 does not change anything in the damping of the solution of equation (9). Compared with the eigenfrequencies in Figure 2, the nutation frequency decreases a little and the precession frequency increases a little. The change is small enough to be ignored.

For the velocity cross feedback control, the eigenequation with the low-pass filter (to simplify the problem, only cross terms' phase lag is considered) is given as follows:

$$J_d s^2 - (1 - k_v/(Ts+1)) J_p \omega i s + 0.5kl^2 = 0 \qquad (s = (\xi + i)\omega) \qquad (17)$$

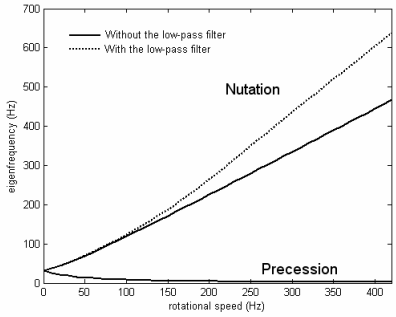

FIGURE 6: Eigenfrequencies in function of the rotational speed (k_v = 0.3).

With the solution of the equation, the eigenfrequencies in function of the rotational speed is shown in Figure 6 (k_v = 0.3, T=0.0005 s). Compared with the eigenfrequencies without the low-pass filter, the

nutation frequency greatly increases while the precession frequency decreases only a little. The damping of the nutation and the damping of the precession is shown in Figure 7.

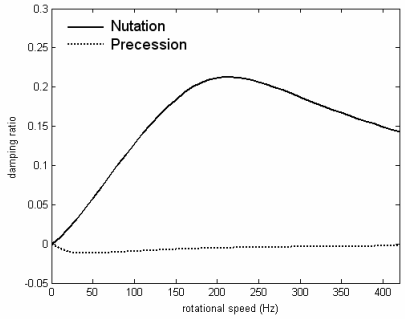

FIGURE 7: Damping of the eigenfrequencies in function of the rotational speed.

In Figure 7, it can be found that the nutation damping of the closed-loop system inceases while the precession damping decreases when the velocity cross feedback control is applied with the low-pass filter considered.

SIMULATION

In the previous sections, the dynamics of the rotor with the different suspension characteristics were discussed, and the closed-loop system will be studied by simulation below. In the simulation, the low-pass filter used is 1/(0.0005s+1), the suspension stiffness is 0.2N/um, the differentiators are as 0.0004s/(0.00002s+1).

Figure 8 gives the bode graph of the closed-loop system running at the rotational speed of 390 Hz.

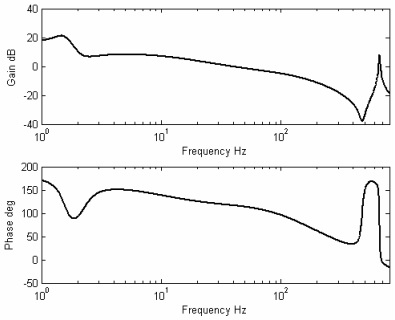

FIGURE 8: Bode graph of the close-loop system running at the rotational speed of 390 Hz.

Figure 8 shows that the high frequency peak is about 663 Hz and the low frequency peak is below 2 Hz. Therefore, the ratio of the high frequency peak position to the synchronous frequency position is about 1.7. It is higher than the ratio shown in Figure 2.

The closed-loop system was simulated at different rotational speeds, and the curves in Figure 9 show the relationship between the peak values and the rotational speed. It is shown that the high frequency peak position of closed-loop systems is markedly higher than the nutation frequency position in Figure 2 at the same rotational speed, whereas the low frequency peak position differs only a little from the precession position in Figure 2.

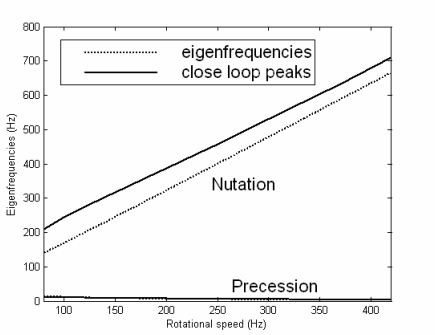

FIGURE 9: Peak positions in function of the rotational speed.

EXPERIMENT

After the dynamics analysis in the different conditions above, some related experimental results will be provided in the subsequent sections--the experimental results about how the nutation and the precession cause system instability, the effects of the velocity cross feedback control and the displacement cross feedback control have been given in a previous paper [9].

In the system, the rotor surface is not so perfect smooth because of machining limitation, and there are harmonic noise caused by electronic parts of the system. The sensor runout was severe, and obvious resonance peaks of double-synchronous frequency and tri-synchronous frequency could be observed in FFT curves of displacement sensor signals when the rotor ran. Sometimes, high order peaks were even higher than the synchronous frequency peak at high rotational speeds. It is shown in Figure 10:

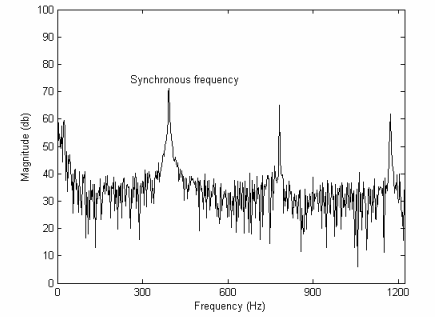

FIGURE 10: FFT curve of a radial displacement sensor signal gotten when the rotor runs.

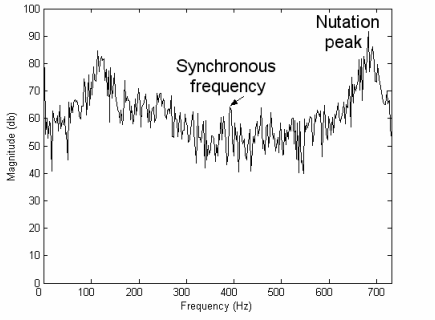

FIGURE 11: Result of the lost stability experiment at the rotation speed of 393 Hz.

The real damping of the nutation was poor when the rotor ran at high rotational speeds and the nutation frequency was near the double-synchronous frequency even when the velocity cross feedback control was applied. The sensor runout signals could excite the nutation vibration of

the rotor. It was found that the rotor becomes unstable when the nutation frequency peak in FFT curves was raised. Figure 11 shows the result of the lost stability experiment at the rotation speed of 393 Hz, and it is easy to find the nutation peak about 681 Hz. Therefore, the ratio of the nutation peak position to the rotational speed is about 1.73. This is consistent with the previous analysis about the high frequency peak of the closed-loop system (Figure 4 and Figure 9).

CONCLUSION

For the flywheel rotor supported by AMBs, the phase lag factors and the controllers greatly influence the value of its nutation frequency and the damping of the nutation and the precession. The nutation frequency increases to near the double-synchronous frequency and the damping of the nutation becomes poor when the rotor runs at high rotational speeds. Furthermore, the sensor runout signals can excite the nutation vibration of the rotor and make the rotor unstable. In controller designs, to ensure that the rotor can run stable at high rotational speeds, the nutation resonance peak of the closed-loop system near double-synchronous frequency should be avoided. At the same time, the sensor runout signals should be restrained.

References

[1] G. Schweitzer, H. Bleuler, A Traxler, “Active Magnetic Bearings — Basics, Properties and Application of Active Magnetic Bearings.,” ETH, Switzerland: Hochschulverlag AG, 1994

[2] M. S. de Queiroz, D. M. Dawson, “Nonlinear Control of Active Magnetic Bearings: A Backstepping Approach,” in IEEE Transactions on Control Systems Technology, vol. 4, no. 5, September 1996, pp. 545-552

[3] K. Nonami, T. Ito, “μ Synthesis of Flexible Rotor-Magnetic Bearing Systems,” in IEEE Transactions on Control Systems Technology, vol. 4, no. 5, September 1996, pp. 503-512.

[4] M. Hirata, T. Ohno, and K. Nonami, “Robust Control of a Magnetic Bearing System using Constantly Scaled H_∞ Control.,” in The 6th International Symposium on Magnetic Bearings, 1998, pp. 713～722.

[5] L. A. Hawkins, B. T. Murphy, J. Kajs, “Analysis and Testing of a Magnetic Bearing Energy Storage Flywheel with Gain-scheduled, MIMO Control,” the 45th ASME International Gas Turbine & Aeroengine Proceedings of ASME TURBOEXPO 2000, Munich Germany, 2000. 1~8

[6] T. J. Park, Y. Kanemitsu, etc., “Identification of Unbalance and High Order Sensor Runout on Rigid Rotor Supported by Magnetic Bearings,” in: Okada Y, Nonami K, eds. Proc. of the 8th International Symposium on Magnetic Bearings. Mito: University of Ibaraki, 2002. 355~360

[7] Y. E. Zhong, Y. Z. He, Z. Wang, "Rotor Dynamics," Tsinghua: Technomic Publishing Co., 1987 (In Chinese)

[8] S.H. Jia, “Rigid Dynamics,” Higher Education Publishing Co., 1987 (In Chinese)

[9] L. Zhao, K. Zhang, R. S. Zhu, H. B. Zhao, “Experimental Research on a Momentum Wheel Suspended by Active Magnetic Bearings,” in: Okada Y, Nonami K, eds. Proc. of the 8th International Symposium on Magnetic Bearings. Mito: University of Ibaraki, 2002. 605~609

[10] M. Ahrens, L. Kucera, “Cross Feedback Control of a Magnetic Bearing System Controller Design Considering Gyroscopic Effects,” Networks [Online]. Available: www.ifr.mavt.ethz.ch